

Study of Chiral Symmetry and $U(1)_A$ using Spatial Correlators for $N_f = 2 + 1$ QCD at finite temperature with Domain Wall Fermions

David Ward¹

S. Aoki, Y. Aoki, H. Fukaya, S. Hashimoto, I. Kanamori, T. Kaneko, Y. Nakamura, C. Rohrhofer, K. Suzuki – JLQCD Collaboration

¹Department of Physics
Osaka University

July 31, 2023

Table of Contents

- 1 Project Overview
- 2 Mesonic Correlators and Spatial Correlators
- 3 Emergence of $SU(2)_{CS}$
- 4 Spatial Correlations and Symmetries on the lattice
- 5 Comparison symmetries between $N_f = 2 + 1$ and $N_f = 2$
- 6 Conclusion

In this talk we discuss the mesonic spatial correlators of $N_f = 2 + 1$ QCD at high T and the associated symmetries measurable through the screening mass difference.

- JLQCD simulates 2+1-flavor QCD at temperatures in the range $136\text{MeV} - 204\text{MeV}$ with Mobius domain-wall quarks with residual masses $< 1\text{MeV}$ with which the $SU(2)_L \times SU(2)_R$ as well as $U(1)_A$ symmetries are well defined.
- The range of quark masses covers from physical up-down quarks to 30MeV .
- The spatial correlator $C_\Gamma(z)$ is relevant to understanding the behavior of the $SU(2)_L \times SU(2)_R$, $U(1)_A$ above and below T_C .
- We compare our result with our previous $N_f = 2$ study [JLQCD 2020].
- We also discuss the emergent $SU(2)_{CS}$ symmetry, which appears at the leading order of the heavy Matsubara mass expansion.

Related talks by JLQCD members

- Characterizing Strongly Interacting Matter at Finite Temperature: (2+1)-Flavor QCD with Mobius Domain Wall Fermions (Earlier talk by Jishnu Goswami).
- Exploring the QCD phase diagram with three flavors of Mobius Domain Wall Fermions (Preceding talk by Yu Zhang).
- Axial $U(1)$ symmetry near the pseudocritical temperature in $N_f = 2 + 1$ QCD above Critical Temperature (Following talk by Kei Suzuki).
- Chiral Susceptibility and axial $U(1)$ anomaly near the (pseudo-)critical temperature (Tomorrow's talk by Hidenori Fukaya).

Acknowledgements

All of this work was done on the following:

Fugaku (hp200130, hp210165, hp210231, hp220279)

Oakforest-PACS

HPCI projects : [hp170061, hp180061, hp190090, hp200086, hp210104]

MCRP in CCS

U. Tsukuba : xg17i032 and xg18i023

Wisteria/BDEC-01 [HPCI: hp220093, MCRP: wo22i038]

Mesonic Correlators

- We consider the flavor triplet bilinear quark operators:

$$\mathcal{O}(x) = \bar{q}(x) \left(\Gamma \otimes \frac{\vec{\tau}}{2} \right) q(x).$$

Here τ^a is an element of the generators of $SU(2)$.

- We measure the spatial correlator through:

$$C_\Gamma(z) = \int_{-\infty}^{\infty} dx \int_{-\infty}^{\infty} dy \int_0^\beta d\tau \langle O_\Gamma(z, x, y, \tau) O_\Gamma^\dagger(0) \rangle$$

On the lattice this becomes

$$C_\Gamma(n_z) = \sum_{n_y, n_x, n_t} \langle O_\Gamma(n_z, n_x, n_y, n_t) O_\Gamma^\dagger(0, 0, 0, 0) \rangle.$$

Mesonic Spatial Correlators and Operators

Γ	Reference Name	Abbr.	Associated Symmetry	
\mathbb{I}	Scalar	S	$U(1)_A$	
γ_5	Pseudo Scalar	PS	$U(1)_A$	
γ_k	Vector	V	$SU(2)_L \times SU(2)_R$	} $SU(2)_{CS}?$
$\gamma_k \gamma_5$	Axial Vector	A		
$\gamma_k \gamma_3$	Tensor	T	$U(1)_A$	
$\gamma_k \gamma_3 \gamma_5$	Axial Tensor	X		

- $\mathcal{O}(x) = \bar{q}(x)(\Gamma \otimes \frac{\tau}{2})q(x)$
- For our purpose we will fix to spatial mesonic correlation functions along the z-axis and study the screening masses[Laine et al. 2004, Cheng et al. 2011, Czerski et al. 2012, HoTQCD 2019, Dalla Brida et al. 2021].

$$\langle \mathcal{O}(t)\mathcal{O}(0) \rangle \rightarrow \langle \mathcal{O}(z)\mathcal{O}(0) \rangle$$

Emergence of $SU(2)_{CS}$ for heavy Matsubara frequency

- Beginning with the free quark Lagrangian:

$$\mathcal{L} = \bar{q}(x)(i\not{D} + m)q(x).$$

- The associated propagator in the z -direction with fixed p_2 and p_1 :

$$\begin{aligned}\langle \bar{q}(z)q(0) \rangle(p_1, p_2) &= \sum_{p_0} \int_{-\infty}^{\infty} \frac{dp_z}{(2\pi)} \frac{m - (i\gamma_0 p_0 + i\gamma_i p_i)}{p_0^2 + \delta_{ij} p_i p_j + m^2} e^{ip_3 z} \\ &= \sum_{p_0} \frac{m + \gamma_3 E - i\gamma_0 p_0 - i\gamma_1 p_1 - i\gamma_2 p_2}{2E} e^{-Ez}\end{aligned}$$

where $E = \sqrt{p_0^2 + m^2 + p_1^2 + p_2^2}$.

Emergence of $SU(2)_{CS}$ for heavy Matsubara frequency

For lattices with $T \gg m^2 + p_1^2 + p_2^2$ we can expand the propagator in terms of $1/T$:

$$\langle \bar{q}(z)q(0) \rangle = \gamma_3 \frac{1 + i \text{sgn}(p_0) \gamma_0 \gamma_3}{2} e^{-\pi Tz} + O(1/T)$$

This quark propagator is invariant under the set of transformations:

$$\begin{aligned} q(x) &\rightarrow e^{i\Sigma^a \theta^a} q(x) \\ \bar{q}(x) &\rightarrow \bar{q}(x) \gamma_0 e^{i\Sigma^a \theta^a} \gamma_0 \end{aligned}$$

where

$$\Sigma = \begin{bmatrix} \gamma_5 \\ \gamma_1 \\ \gamma_2 \end{bmatrix}$$

forms the so-called chiral spin $SU(2)_{CS}$ group [Glozman 2015, Glozman and Pak 2015, 2017, Rohrhofer et al. 2017, 2019, 2020, Lattice 2019].

Simulating $N_f = 2 + 1$ QCD

- $N_f = 2 + 1$ QCD with Mobius domain wall quarks with $m < 1\text{MeV}$ and Symanzick gauge action.
- $a^{-1} = 2.453\text{GeV}$
- $L = 32$ (2.58fm)
- m_{ud} from $\sim 4.9\text{MeV}$ to 30MeV
- m_s at physical mass pt.
- Temperature ranges from $T = 136\text{MeV} - 204\text{MeV}$.
- psuedo $T_c \sim 150\text{MeV}$

$L^3 \times L_t$	β	$T(\text{MeV})$	am	$m(\text{MeV})$
$32^3 \times 12$	4.17	204	0.0020	4.9
$32^3 \times 12$	4.17	204	0.0035	8.6
$32^3 \times 12$	4.17	204	0.0070	17
$32^3 \times 12$	4.17	204	0.0120	29
$32^3 \times 14$	4.17	175	0.0020	4.9
$32^3 \times 14$	4.17	175	0.0035	8.6
$32^3 \times 14$	4.17	175	0.0070	17
$32^3 \times 14$	4.17	175	0.0120	29
$32^3 \times 16$	4.17	153	0.0020	4.9
$32^3 \times 16$	4.17	153	0.0035	8.6
$32^3 \times 16$	4.17	153	0.0070	17
$32^3 \times 16$	4.17	153	0.0120	29

Effective Mass and Fit

- In our determinations of the mass spectrum we make use of the the $\cosh(z)$ fitting ansatz.
- Symmetries are drawn from the difference in the screening masses between channels related by associated Chiral transformation. i.e.

$$\text{For } SU(2)_L \times SU(2)_R : \quad \Delta M = |m_{eff}^{Ax} - m_{eff}^{Vx}|$$

$$\begin{aligned} \text{For } U(1)_A : \quad \Delta M_\pi &= |m_{eff}^{PS} - m_{eff}^S| \\ \Delta M &= |m_{eff}^{Xt} - m_{eff}^{Tt}| \end{aligned}$$

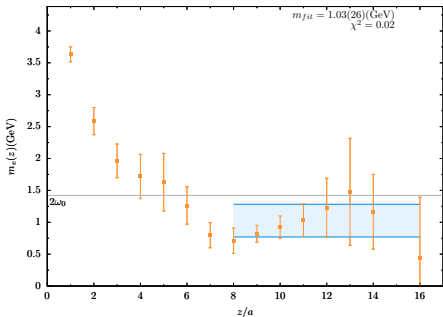
$$\text{For } SU(2)_{CS} : \quad \Delta M = |m_{eff}^{Vx} - m_{eff}^{Xt}|$$

- In addition to fitting errors we also check for symmetry breaking by taking the proportion of $\Delta M/M$ where M is the larger of the masses produced by fitting.

Effective Mass and Fit Range

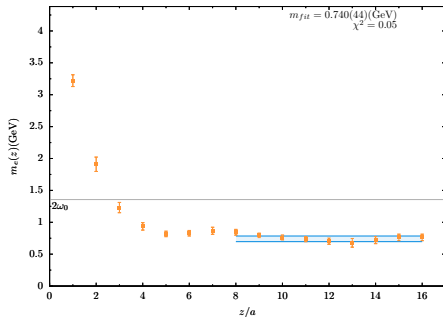
S

4.9 MeV Quark Mass : Effective Mass and Fit for *S* Channel



PS

4.9 MeV Quark Mass : Effective Mass and Fit for *PS* Channel



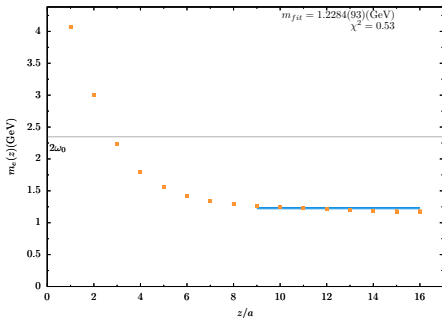
$T = 204 \text{ MeV}$ at $m_{ud} = 4.9 \text{ MeV}$

Effective Mass and Fit Range

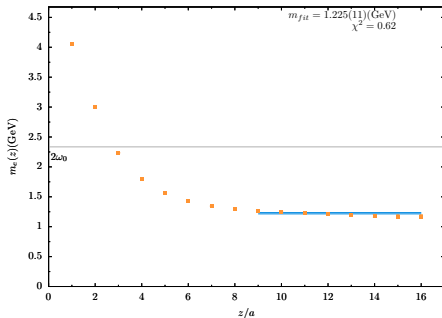
Ax

Vx

4.9 MeV Quark Mass : Effective Mass and Fit for Ax Channel



4.9 MeV Quark Mass : Effective Mass and Fit for Vx Channel

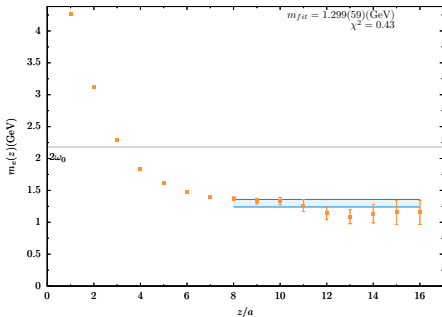


$T = 204 \text{ MeV}$ at $m_{ud} = 4.9 \text{ MeV}$

Effective Mass and Fit Range

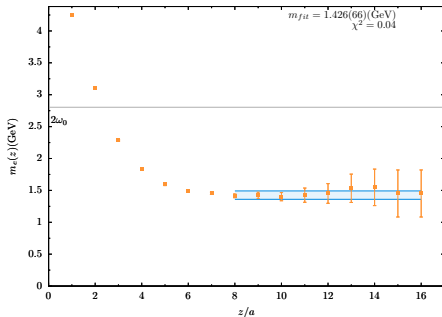
Xt

4.9 MeV Quark Mass : Effective Mass and Fit for Xt Channel



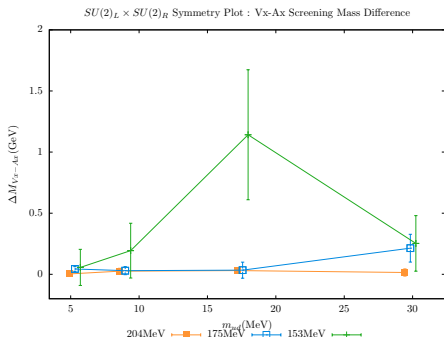
Tt

4.9 MeV Quark Mass : Effective Mass and Fit for Tt Channel



$T = 204\text{MeV}$ at $m_{ud} = 4.9\text{MeV}$

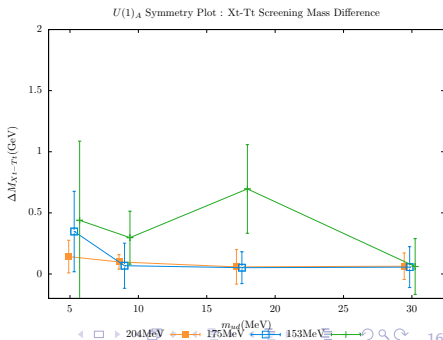
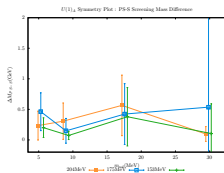
$SU(2)_L \times SU(2)_R$ symmetry



- For temperatures above 175MeV and 204MeV we see the restoration of the chiral symmetry within error, $\Delta M/M \sim 5\%$.
- For 153MeV chiral symmetry is intact for m_{ud} around physical mass $\Delta M/M \sim 4\%$. For all other masses chiral symmetry is broken.

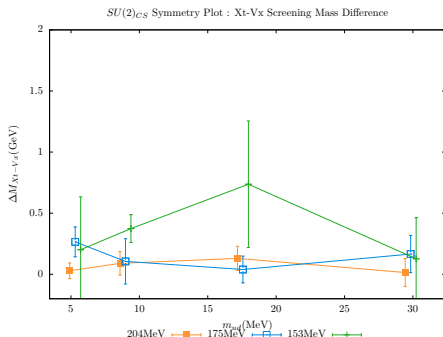
$U(1)_A$ symmetry

- We will omit the PS-S due to the noisy scalar channel.
- For Xt-Tt, at 204MeV the symmetry looks good with $\Delta M/M \sim 5 - 12\%$ on average.
- For 153MeV the symmetry is broken, which appears consistent with the $U(1)_A$ susceptibility.

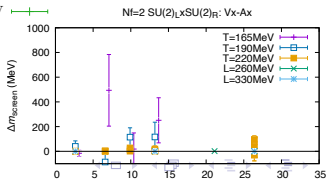
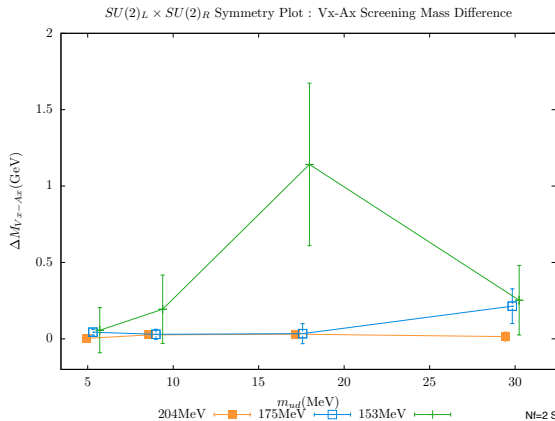


$SU(2)_{CS}$ symmetry

- Temperatures 204MeV is consistent for both $A_x\text{-}X_t$ and $X_t\text{-}V_x$ with $\Delta M/M \sim 10\%$.
- At 175MeV the symmetry appears the same with the exception of the lightest quark mass.
- 153MeV is broken within errors across both plots, and both share large $\Delta M/M$ of about $50\%+$ (but with large errors).

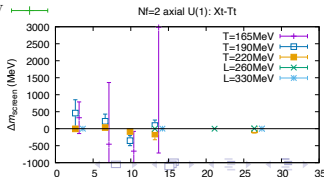
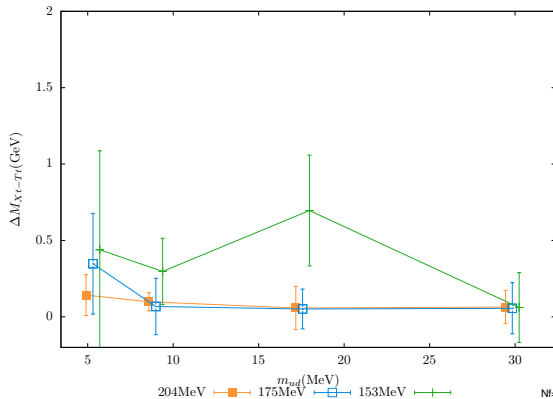


Comparison with $N_f = 2$ Symmetries



Comparison with $N_f = 2$ Symmetries

$U(1)_A$ Symmetry Plot : Xt-Tt Screening Mass Difference



Conclusions

- Based on the screening mass differences we can see a restoration of the $SU(2)_L \times SU(2)_R$ symmetry above the pseudocritical temperature $T_c \sim 153\text{MeV}$ at the physical point.
- Likewise we also observe suppression of the $U(1)_A$ symmetry breaking at the same temperatures.
- In addition to this we observe that $SU(2)_{CS}$ symmetry becomes good at $T = 204\text{MeV} \sim 1.3T_c$. (broken at $T = 153, 175\text{MeV}$).